



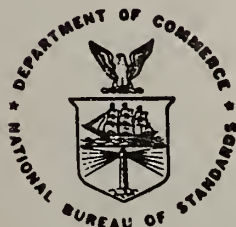
A11106 979532

NBSIR 82-2622

The Development of Hazardous Conditions in Enclosures With Growing Fires

U.S. DEPARTMENT OF COMMERCE
National Bureau of Standards
National Engineering Laboratory
Center for Fire Research
Washington, DC 20234

December 1982



QC

100

U56

82-2622

1982

C.2

U.S. DEPARTMENT OF COMMERCE

NATIONAL BUREAU OF STANDARDS

FEB 2 1983

Not a copy
2000
JES
82-2622
1982
0.2

NBSIR 82-2622

**THE DEVELOPMENT OF HAZARDOUS
CONDITIONS IN ENCLOSURES WITH
GROWING FIRES**

Leonard Y. Cooper

U.S. DEPARTMENT OF COMMERCE
National Bureau of Standards
National Engineering Laboratory
Center for Fire Research
Washington, DC 20234

December 1982

U.S. DEPARTMENT OF COMMERCE, Malcolm Baldrige, *Secretary*
NATIONAL BUREAU OF STANDARDS, Ernest Ambler, *Director*

TABLE OF CONTENTS

| | Page |
|--|------|
| LIST OF FIGURES | iv |
| NOMENCLATURE | v |
| Abstract | 1 |
| INTRODUCTION | 1 |
| A DESCRIPTION OF THE MODEL AND ITS GOVERNING EQUATIONS | 3 |
| The Model | 3 |
| The Governing Equations | 4 |
| Discussion of the Equations | 6 |
| Solutions From Ignition to τ_0 | 6 |
| Solutions From Time τ_0 to the Time When $\zeta = -\delta$ | 9 |
| Solution for ϕ When $\zeta = -\delta$ | 10 |
| USING THE SOLUTIONS TO PREDICT FIRE ENVIRONMENTS | 10 |
| A Problem in Smoldering Combustion | 10 |
| Hazard Development in Enclosures Containing Some Larger Scale Fires | 13 |
| SUMMARY AND CONCLUSIONS | 15 |
| ACKNOWLEDGMENTS | 16 |
| REFERENCES | 17 |

LIST OF FIGURES

| | Page |
|--|------|
| Figure 1. Fire-in-enclosure flow dynamics consistent with the model | 19 |
| Figure 2. Plots of $\zeta(\tau)$ for different values of n and ε , $0 < \tau \leq \tau_0$ | 20 |
| Figure 3. Plots of $\varepsilon^{2(n+3)/[3(3n+5)]} \tau_0$ and ϕ_0 as functions of $1/\varepsilon$ for different values of n | 21 |
| Figure 4. Plots of $\zeta(\sigma)$ and $\phi(\sigma)$, $0 \leq \zeta < 1$, for different values of ε , and for $n = 0$, $n = 1$, and $n = 2$ | 22 |
| Figure 5. Plots of $\sigma_0(\varepsilon)$ and $\phi_0(\varepsilon)$ for different values of n | 23 |
| Figure 6. Plots of $\zeta(\sigma)$ and $\phi(\sigma)$, $-\delta < \zeta \leq 0$, for different values of σ_0 | 24 |
| Figure 7. Plots of $\zeta(\sigma)$ and $\phi(\sigma)$, $\zeta \leq 0$, for different values of σ_0 , and for $\delta = 0$, $\delta = 0.2$, and $\delta = 0.4$ | 25 |
| Figure 8. Plots of $\zeta(\sigma)$ and $\phi(\sigma)$ for $n = 1$ and $\varepsilon = 0.00016$, and plots of μ_{CO} data from cotton and polyurethane smoldering experiments | 26 |

NOMENCLATURE

| | |
|----------------|---|
| A | enclosure floor area |
| ASET | available safe egress time |
| B | a constant |
| b | a constant |
| \dot{C} | combustion product generation rate |
| \dot{C}_{CO} | CO generation rate |
| C_p | specific heat at constant pressure |
| f | a function |
| g | acceleration of gravity |
| H | fire-to-ceiling distance |
| H_c | heat of combustion |
| M | combustion product concentration |
| \dot{m} | mass loss rate |
| n | an integer |
| \dot{Q} | energy release rate |
| \dot{Q}_o | a characteristic energy release rate |
| \dot{Q}_o^* | dimensionless \dot{Q}_o |
| R | ratio of leading terms in a ζ expansion |
| RSET | required safe egress time |
| T | upper layer temperature |
| T_a | ambient temperature |
| t | time |
| t_o | value of t when $Z_1 = 0$ |
| t_{DET} | time at detection |
| t_{HAZ} | time at hazard |

| | |
|---------------|---|
| u_c | dimensional unit of a combustion product |
| Z_1 | elevation of interface above fire |
| α | a constant of proportionality |
| β | a constant of proportionality |
| γ | ratio of mass of CO generated to mass of material |
| Δ | elevation of fire above floor |
| δ | Δ/H |
| ϵ | a dimensionless parameter |
| ζ | Z_1/H |
| $\zeta^{(n)}$ | nth term in a ζ expansion |
| λ_c | fraction of \dot{Q} transferred to enclosure surfaces |
| λ_r | fraction of \dot{Q} radiated from combustion zone |
| μ | dimensionless M |
| ρ_a | ambient density |
| σ | dimensionless t |
| σ_0 | dimensionless t_0 |
| τ | dimensionless t |
| τ_0 | dimensionless t_0 |
| ϕ | T/T_a |
| ϕ_0 | value of ϕ at $t = t_0$ |

THE DEVELOPMENT OF HAZARDOUS CONDITIONS
IN ENCLOSURES WITH GROWING FIRES

Leonard Y. Cooper

Abstract

A mathematical model for simulating the environment in enclosures during the growth stage of hazardous fires was developed previously. To use the model one must specify the energy release rate of the fire, certain heat transfer parameters, the area and height of the enclosure and the elevation of the fire above the floor. Solution to the model's equations would yield the time-varying thickness, temperature, and product of combustion concentrations of an upper smoke layer which starts to drop from the enclosure ceiling at the time of ignition. In this paper the model equations are solved for the general class of fires whose energy release rate, \dot{Q} , and product of combustion generation rates, \dot{C} , are approximately proportional to t^n (t is time and $n \geq 0$). For such fires, general results for the complete solution history of the enclosure environment are obtained and presented in the form of graphs, and, where possible, by closed form analytic expressions. Use of the results is illustrated in two example problems. The first of these involves a problem in smoldering combustion where, according to experimental data, the combustion zone can be simulated by an $n = 1$ fire. The second involves a prediction of the environment produced in an enclosure which contains an $n = 2$ fire, which simulates a specific, large-scale, flaming fire hazard.

INTRODUCTION

An excess of available safe egress time (ASET) over required safe egress time (RSET) as a criterion for life safety in buildings under fire conditions is a concept which has been introduced in references 1-4. ASET is the interval between the time of fire detection (and successful occupant alarm), t_{DET} , and the time of onset of hazardous conditions, t_{HAZ} , i.e., $ASET = t_{HAZ} - t_{DET}$. RSET is the actual time required for occupants to evacuate from threatened spaces. If the life safety criterion is to be used in an evaluation of the safety of an existing building or of a tentative building design, then estimates of ASET and RSET under characteristic potential fire scenarios must be obtained.

An estimate of ASET requires estimates of t_{DET} and t_{HAZ} . t_{DET} depends on the characteristics of available detection and alarm devices, and, in general, on the interactions of these with fire generated environments which develop around them. Besides depending on the physiological characteristics of occupants, t_{HAZ} also depends on the fire environment. It is therefore evident that estimates of t_{DET} and t_{HAZ} require predictions of the dynamic environment which develops in buildings during fire conditions. The capability of providing such predictions under a wide variety of fire scenarios is a general goal of enclosure fire modeling.

A relatively simple model which predicts the dynamic fire conditions in compartments of fire origin has been proposed in references 1 and 2. Besides the height and floor area of the compartment and the elevation of the fire above the floor, the free burn characteristics of the fuel assembly in which the potential fire originates is a required input to the model. (Free burn is defined as a burn of the fuel assembly in a large ventilated space which contains a relatively quiescent atmosphere.) The model has been shown to provide useful analytic simulations of fire conditions in single room enclosures and in one-level, freely connected, multiroom enclosures where the overall external boundaries of the enclosures were sealed except for leakage paths near the floor^{2,5}. The model is capable of giving excellent results up to and beyond the onset of hazardous conditions.

While the model involves governing equations that are easily solved with the use of a computer, it does not lend itself to generalized solutions which can be displayed "once and for all" by charts, graphs or tables. Nevertheless, for any specific fire [i.e., for a fire of specified free burn energy release, $\dot{Q}(t)$, and product of combustion generation rate, $C(t)$, where t is time] solutions to the model's equations for arbitrary enclosure height and area and for arbitrary fire elevation can indeed be obtained and displayed. It is the purpose of the present work to solve the governing equations for the broad class of fires whose \dot{Q} can be reasonably approximated by growth proportional to t^n (for arbitrary $n \geq 0$), and whose \dot{C} 's of interest can be reasonably approximated by growth proportional to \dot{Q} .

A DESCRIPTION OF THE MODEL AND ITS GOVERNING EQUATIONS

The Model

A rational basis for the following idealized description of real enclosure fires as well as a development of the subsequent equations are presented at length in references 1 and 2. Figure 1 depicts the developing fire conditions.

A fire located a distance H below the ceiling is initiated in an enclosure of area A . The ambient conditions in the enclosure are described by the density, ρ_a , the specific heat at constant pressure, C_p , and the absolute temperature, T_a . The fire is located at an elevation, Δ , above the floor (i.e., the total height of the enclosure is $H + \Delta$). An estimate of the total energy release rate of the fire, \dot{Q} , is assumed to be available, as are the fire's generation rates, the \dot{C} 's, of any products of combustion of interest. In practice it is recommended that free burn heat release rates and product of combustion generation rates be used as surrogates for \dot{Q} and the \dot{C} 's, respectively. This recommendation is consistent with the fact that onset of hazardous conditions within the enclosure will occur at temperature and combustion product concentration levels which are low compared to those levels at which variations from free burn will begin to be significant.

As the fire develops from ignition at $t = 0$, buoyancy forces drive the high temperature products of combustion upward toward the ceiling. In this way a plume of upward moving elevated temperature gases is formed above the fire. All along the axis of the plume, relatively quiescent and cool ambient air is laterally entrained and mixed with the plume gases as they continue their ascent to the ceiling. As a result of this entrainment the total mass flow rate in the plume continuously increases and the average temperature and average concentration of products of combustion in the plume continuously decreases with increasing height.

When the plume gases impinge on the ceiling they spread across it forming a relatively thin, stably stratified upper layer. As the upward filling process continues, the upper gas layer grows in depth, and the relatively sharp interface between it and the cool ambient air layer below continuously drops.

With regard to the disposition of \dot{Q} , it is assumed that $\lambda_r \dot{Q}$ is the net amount which is actually radiated from the fire's combustion zone while the remainder, $(1-\lambda_r)\dot{Q}$, is convected upward. It is assumed, further, that $\lambda_c \dot{Q}$ is the net rate at which energy is transferred to the internal bounding surfaces of the enclosure. $\lambda_c \dot{Q}$ includes all heat transfer to surfaces by both convection and radiation. Reference 2 recommends choosing $\lambda_r = 0.35$ for typical hazardous flaming fires while λ_c typically varies in a range of 0.6-0.9, depending on enclosure geometry, the fire's proximity to walls, and on the value of λ_r .

At every instant, it is assumed that the gases in the upper layer are fully mixed. Accordingly, the model provides a time-dependent description of the environment in the enclosure by predicting the elevation, $Z_1(t)$, of the interface above the fire, and the absolute temperature, $T(t)$, and combustion product concentration, $M(t)$, of the upper layer. If the dimensions of \dot{C} are taken to be u_c per unit time, where u_c is a dimensional unit appropriate for the particular combustion product, then the dimension of M is the average amount of product (dimension u_c) per unit mass of upper layer mixture.

There are basically two mechanisms for the increase of the upper layer volume (decrease of Z_1). The first is a result of significant rates of mass injection from the plume into the upper layer on account of entrainment (mass addition from the fuel itself is assumed to be negligible). The second mechanism is a result of gas expansion due to energy transfer from the fire to the gas. This comes about because relatively low density (high temperature) upper layer gases replace relatively high density (ambient temperature) air, with a net efflux of ambient air from assumed floor level leakage points. As the interface drops from the ceiling its downward velocity is continuously reduced. The entrainment mechanism, which is totally dominant early in the fire, eventually becomes small compared to the expansion mechanism. By the time $Z_1 = 0$ and the interface drops below the fire (if $\Delta \neq 0$), only the expansion mechanism remains viable for further reductions in Z_1 .

The Governing Equations

For arbitrarily specified \dot{Q} and \dot{C} , the initial value problem for Z_1 , T , and M is presented in reference 2. Here, fire scenarios which develop from a

specific class of \dot{Q} and \dot{C} , namely, $\dot{Q} \sim t^n$ and $\dot{C} \sim \dot{Q}$ are being investigated. To be definite, it is assumed that \dot{Q} and \dot{C} of free burn fires of interest can be approximated by

$$\dot{Q}(t) = \dot{Q}_0 [tH^{3/2}g^{1/2}/A]^n; \dot{C}(t) = \beta\dot{Q}(t) \quad (1)$$

where \dot{Q}_0 represents a characteristic energy release rate, n is any non-negative number, β is a constant of appropriate dimension, and g is the acceleration due to gravity.

It turns out to be convenient to introduce the following dimensionless variables and parameters

$$\begin{aligned} \zeta &= Z_1/H \quad (\text{interface elevation}) \\ \phi &= T/T_a \quad (\text{upper layer temperature}) \\ \mu &= (1-\lambda_c)M/(\beta C_p T_a) \quad (\text{upper layer product concentration}) \\ \tau &= 3[(1-\lambda_r)\dot{Q}_0^*]^{1/3} (tH^{3/2}g^{1/2}/A)^{(n+3)/3}/(n+3) \quad (\text{time}) \\ \varepsilon &= (1-\lambda_c)[(n+3)/3]^{2n/(n+3)} \dot{Q}_0^{*2/(n+3)}/(1-\lambda_r)^{(n+1)/(n+3)} \quad (\text{fire strength}) \\ \dot{Q}_0^* &= \dot{Q}_0/(\rho_a C_p T_a g^{1/2} H^{5/2}) \quad (\text{characteristic energy release rate}) \\ \delta &= \Delta/H \quad (\text{fire elevation}) \end{aligned} \quad (2)$$

Using the above definitions in the model equations of reference 2 eventually leads to the following equations for ζ , ϕ , and μ :

$$\frac{d\zeta}{d\tau} = \begin{cases} -\varepsilon\tau^{2n/(n+3)} - 0.210\zeta^{5/3}; & 0 < \zeta \leq 1 \\ -\varepsilon\tau^{2n/(n+3)}; & -\delta < \zeta \leq 0 \\ 0; & \zeta = -\delta \end{cases} \quad (3)$$

$$\phi = \{1 - (n+3)\varepsilon\tau^{3(n+1)/(n+3)}/[3(n+1)(1-\zeta)]\}^{-1}; \quad -\delta < \zeta \leq 1 \quad (4)$$

$$\frac{d\phi}{d\tau} = \varepsilon\phi\tau^{2n/(n+3)}/(1+\delta); \quad \zeta = -\delta$$

$$\mu = \phi - 1; \quad -\delta \leq \zeta \leq 1 \quad (5)$$

where Eq. (3) must be solved subject to

$$\zeta(\tau=0) = 1 \quad (6)$$

and where early time estimates for ζ , ϕ and μ are

$n = 0$:

$$\lim_{\tau \rightarrow 0} (\zeta-1)/(1+\varepsilon/0.210) = -0.210\tau + \text{higher order terms in } \tau \quad (7)$$

$$\lim_{\tau \rightarrow 0} \phi/(1+\varepsilon/0.210) = \lim_{\tau \rightarrow 0} (\mu+1)/(1+\varepsilon/0.210) = 1 + 5\varepsilon\tau/6 + \text{higher order terms in } \tau$$

$n > 0$:

$$\lim_{\tau \rightarrow 0} (\zeta - 1) = -0.210\tau + \text{higher order terms in } \tau \quad (8)$$

$$\lim_{\tau \rightarrow 0} (\phi - 1) = \lim_{\tau \rightarrow 0} \mu = (n+3)\epsilon\tau^{2n/(n+3)} / [3(n+1)(0.210)] + \text{higher order terms in } \tau$$

Eq. (3) describes the rate of descent of the interface as it passes through the regions above the fire ($0 < \zeta < 1$), below the fire ($-\delta < \zeta < 0$), and at the floor ($\zeta = -\delta$). Eqs. (4) and (5) describe the corresponding upper layer temperature and product concentration. Eqs. (7) and (8) are useful in starting a numerical solution to Eqs. (3) and (4).

Discussion of the Equations

The last section presented the equations which govern the dynamics of ζ , ϕ and μ . From Eq. (5) the solution for μ would follow directly from the solution for ϕ . From the time of ignition to the time that the interface drops to the floor of the enclosure, a solution for ϕ could be obtained from Eqs. (4), (7) and (8) provided a solution for ζ was available. Beyond that time the solution for ϕ could be continued by a direct integration of the second of Eq. (4).

With the above observations, attention is drawn to the solution for ζ . From ignition until the time, $\tau_0 = \tau(\zeta=0)$, when the interface drops to $\zeta = 0$, ζ is governed by Eq. (6) and the first of Eq. (3). No general closed form solution is possible, and a numerical solution for $\zeta(\tau; \epsilon, n)$ is in order. Once this has been obtained, the solution can be extended beyond τ_0 by direct integration of the second and third of Eq. (3).

Solutions From Ignition to τ_0

In general there is no particular problem in obtaining a numerical integration for ζ . However, in terms of generating a display of working graphical solutions which include times when ζ is small and positive, a problem does arise in the limit as $\epsilon \rightarrow 0$. Applying such a limit to the first of Eq. (3) leads, in a first approximation, to the total neglect of the earlier referenced (left hand) expansion term in comparison to the (right hand) entrainment term. This corresponds, physically, to the situation of an interface that approaches

the elevation of the fire asymptotically in time. This is the incompressible limit of a heat (buoyancy) source in an enclosure studied for the $n = 0$ case by both Baines and Turner⁶ and Zukoski⁷. In the present nomenclature, and for a source whose strength grows as t^n , this incompressible solution is simply found to be

$$\zeta(\tau; \epsilon=0, n) \equiv \zeta^{(0)}(\tau) = [1 + 0.210(2/3)\tau]^{-3/2} \quad (9)$$

This result is plotted in Figure 2 along with other numerically obtained, nonzero ϵ solutions for ζ .

The above result for $\epsilon = 0$ leads to the result that $\zeta \rightarrow 0$ as $\tau \rightarrow \infty$. But, for a fixed n and an arbitrarily small but nonzero ϵ , a $\zeta = 0$ position of the interface will in fact be attained at some finite, large τ . Thus, there will be no uniformly valid solution for $\zeta(\tau; \epsilon, n)$ in a neighborhood of $\zeta = 0$ which is independent of ϵ in the limit $\epsilon \rightarrow 0$. Away from the $\zeta = 0$ point, however, such a uniformly valid solution does exist, i.e., for ζ in the range $0 < B \leq \zeta \leq 1$, and for some fixed B ,

$$\lim_{\substack{\epsilon \rightarrow 0 \\ n \text{ fixed} \geq 0}} \zeta(\tau; \epsilon, n) = \zeta^{(0)}(\tau) [1 + O(\epsilon)] \quad (10)$$

This small ϵ behavior of ζ can be observed in Figure 2.

The small ϵ limit is very important in problems of physical interest. As an example, consider a constant ($n = 0$) smolder source of 0.5 kW located a distance of 2 m below a ceiling and with $\lambda_r = 0.1$ and $\lambda_c = 0.75$. This leads to $\epsilon = 5.3(10^{-4})$. As an example of a relatively strong fire, consider a constant flaming fire of 5,000 kW located .5 m below a ceiling, and with $\lambda_r = 0.35$ and $\lambda_c = 0.75$. This leads to $\epsilon = 6.0(10^{-2})$. In terms of a "small ϵ " criterion, the latter fire is still relatively weak.

From the above discussion it is reasonable to seek a regular perturbation solution for ζ of the form

$$\lim_{\substack{\epsilon \rightarrow 0 \\ 0 \leq \tau \text{ fixed}}} \zeta = \sum_{p=0}^{\infty} \epsilon^p \zeta^{(p)}(\tau; n) \quad (11)$$

for $1 \geq \zeta > 0$, where $\zeta^{(0)}$ has been obtained above. Furthermore, it is reasonable to expect that the useful range of the above expansion can be extended to large τ values which satisfy

$$\left| \varepsilon \zeta^{(p+1)}(\tau; n) / \zeta^{(p)}(\tau; n) \right| \leq b < 1 \quad (12)$$

for all p greater than some fixed value P . Provided ε was small enough, but not identically zero, such large τ values would include the particularly interesting value τ_0 , which corresponds to $\zeta = 0$.

The suggested perturbation analysis was carried out for the first few terms of the Eq. (11) expansion. This leads to

$$\lim_{\tau \rightarrow \infty} \varepsilon \zeta^{(1)} / \zeta^{(0)} = - \frac{2(n+3)}{(11n+21)} (0.410/3)^{3/2} \varepsilon \tau^{3(3n+5)/[2(n+3)]} \equiv -R \quad (13)$$

$$\lim_{\tau \rightarrow \infty} \varepsilon \zeta^{(2)} / \zeta^{(1)} = \frac{5(n+3)}{12(5n+9)} R \quad (14)$$

and the resulting estimate for ζ

$$\lim_{\tau \rightarrow \infty} \left[\lim_{\varepsilon \rightarrow 0} \zeta \right] = \zeta_0(\tau) \left[1 - R + \frac{5(n+3)}{12(5n+9)} R^2 + \dots \right] \quad (15)$$

Applying this estimate at $\zeta = 0$ leads to

$$0 = 1 - R(\tau_0; \varepsilon, n) + \frac{5(n+3)}{12(5n+9)} R^2(\tau_0; \varepsilon, n) + \dots \quad (16)$$

which, together with the Eq. (13) definition of R , suggests the general result

$$\lim_{\varepsilon \rightarrow 0} \varepsilon^{2(n+3)/[3(3n+5)]} \tau_0(\varepsilon; n) = f(n) = 0(1) \quad (17)$$

The $f(n) = 0(1)$ estimate is a result of the fact that the quotients $(n+3)/(11n+21)$ and $(3n+5)/(n+3)$ of Eq. (13) and $5(n+3)/[12(5n+9)]$ of Eq. (14) are relatively insensitive to n in the entire range $0 \leq n < \infty$, the latter of these always having a value of approximately 0.1.

Guided by the tentative result of Eq. (17), numerically computed τ_0, ε pairs were obtained and plotted in Figure 3 for a variety of different n values. The corresponding values for $\phi(\tau_0; \varepsilon, n)$ were also obtained and plotted. The plots of the numerical data are seen to be consistent with the asymptotic result of Eq. (17). Indeed, over a very broad ε range of practical interest the value of the ordinate for a given n is seen to be relatively uniform in ε . For example, in the constant fire case,

$$\varepsilon^{2/5} \tau_0(\varepsilon; n=0) = [(1-\lambda_r)(1-\lambda_c)^2 g_0^3 / (\rho_a C_p T_a)^3]^{1/5} t_0 / A = 4.2(1 \pm 0.15) \quad (18)$$

in the range $0.5(10^{-4}) < \varepsilon < 0.5(10^{-1})$, where t_0 is the value of t when $Z_1 = 0$.

The above observation for $n = 0$ leads to a remarkable practical result; namely, in the case of constant fires, and for fire elevations and room heights of practical interest, the time for a smoke layer to drop from the ceiling to the elevation of the fire is relatively independent of H .

Solutions From Time τ_0 to the Time When $\zeta = -\delta$

This section will be devoted to an analysis of the ζ, ϕ solution beyond the time τ_0 . It is convenient to present results in terms of a new dimensionless time variable, σ , which is defined by

$$\sigma = \frac{(n+3)}{3(n+1)} \epsilon \tau^{3(n+1)/(n+3)} \quad (19)$$

Accordingly, working plots for $\zeta(\sigma)$ and $\phi(\sigma)$ have been numerically generated and plotted in Figure 4 for selected values of n . Also, plots of $\sigma_0(\epsilon;n)$ which correspond to the results of Figure 3 are plotted in Figure 5, where σ_0 is defined as the value of σ when $\tau = \tau_0$.

After the upper layer interface drops to the fire elevation, $\zeta = 0$, its further drop until $\zeta = -\delta$ is determined by the second of Eq. (3) which can be written as

$$\frac{d\zeta}{d\sigma} = -1, \quad -\delta < \zeta \leq 0 \quad (20)$$

where

$$\zeta(\sigma_0) = 0 \quad (21)$$

where σ and σ_0 are defined in Eq. (19), and where $\sigma_0(\epsilon;n)$ is plotted in Figure 5. It is noteworthy that a $\sigma_0 = 1$ estimate of the time for a $\zeta = 1$ to $\zeta = 0$ interface drop corresponds to a result which can be derived from a neglect of the entrainment term of Eq. (3). In this range of ζ , the real rate-of-drop of the interface will be enhanced by entrainment, and, therefore, $\sigma_0 < 1$.

During the times of present interest it is still possible to compute ϕ from the first of Eq. (4), which can be written as

$$\phi = [1 - \sigma / (1 - \zeta)]^{-1}; \quad -\delta < \zeta \leq 0 \quad (22)$$

The solutions for $\zeta(\sigma; \sigma_0)$ and $\phi(\sigma; \sigma_0)$ are

$$\zeta = \sigma_0 - \sigma, \quad \phi = 1 + \sigma / (1 - \sigma_0); \quad -\delta < \zeta \leq 0 \quad (23)$$

and they are plotted parametrically in Figure 6 for different values of $0 \leq \sigma_0 < 1$. In order to use these results to obtain histories for ζ and ϕ for a particular fire scenario one computes ε , finds the value for σ_0 from Figure 5, and then uses the appropriate ζ and ϕ plots of Figure 6 for times in excess of σ_0 , and up until $\zeta = -\delta$.

Solution for ϕ When $\zeta = -\delta$

The parameter δ does not enter into the solutions for ζ or ϕ until $\zeta = -\delta$ at which time the layer has just filled the entire enclosure. The floor level leakage gas changes from ambient air to upper layer gas. Subsequent to this time, ϕ is governed by the second of Eq. (4) which can be rewritten as

$$\frac{d\phi}{d\sigma} = \phi/(1+\delta), \quad \sigma \geq \sigma_0 + \delta \quad (24)$$

For the solution to Eq. (24) to be continuous with the ϕ solution of Eq. (23) it is necessary that

$$\phi(\sigma = \sigma_0 + \delta) = 1 + (\sigma_0 + \delta)/(1 - \sigma_0) \quad (25)$$

The solution to Eqs. (24) and (25) is

$$\phi = [(1+\delta)/(1-\sigma_0)] \exp[(\sigma - \sigma_0 - \delta)/(1+\delta)], \quad \sigma \geq \sigma_0 + \delta \quad (26)$$

Using the results of Eqs. (23) and (26), the solutions for ζ and ϕ as functions of σ with σ_0 as a parameter, and for the δ values 0, 0.2, and 0.4 are plotted in Figure 7.

USING THE SOLUTIONS TO PREDICT FIRE ENVIRONMENTS

The solutions of the last section will now be applied to two example problems. The first example will involve a problem of smoldering combustion where results of the present theory will be compared to some full scale experimental results. The second example will illustrate the use of the theory in predicting the environment produced in an enclosure which contains a specific large-scale flaming fire hazard.

A Problem in Smoldering Combustion

Smoldering experiments reported by Quintiere et al.⁸ were carried out in an enclosure of height 2.44 m and area 8.83 m². The opening to the enclosure was

formed by a closed undercut door where the undercut formed a 0.76 m x 0.025 m open horizontal slit at floor level. A smoldering source was placed in the enclosure where the top surface of the source was at an elevation of 0.33 m. Gas analysis was carried out at four equidistant elevations from the ends of sampling tubes extending horizontally approximately 0.5 m from the walls.

The tests evaluated two different smolder sources; a loosely packed bed of cotton, and blocks of flexible polyurethane foam. Mass loss rates, \dot{m} , were found to be approximately linear in time throughout the first hour of the two tests, i.e.,

$$\dot{m} = \alpha t \quad 0 < t < 60 \text{ min} \quad (27)$$

where

$$\alpha = \begin{cases} 0.21 \text{ g/min}^2 & \text{for polyurethane} \\ 0.33 \text{ g/min}^2 & \text{for cotton} \end{cases}$$

The heats of combustion, H_c , of the materials as well as the ratios, γ , of mass of CO produced to mass of material lost were obtained in a separate small scale apparatus. These were found to be

$$H_c = \begin{cases} (11 \pm 1) \text{ kJ/g}_{\text{cotton}} \\ (15 \pm 8) \text{ kJ/g}_{\text{polyurethane}} \end{cases} \quad (28)$$

$$\gamma = \begin{cases} 0.11 \text{ g}_{\text{CO}}/\text{g}_{\text{cotton}} \\ (0.10 \pm 0.01) \text{ g}_{\text{CO}}/\text{g}_{\text{polyurethane}} \end{cases} \quad (29)$$

The results of the previous section will be used to predict the environment which developed in the enclosure during the course of the two different material evaluations.

Comparing Eqs. (27), (28) and (29) to Eq. (1) leads to

$$\begin{aligned} \dot{Q} &= \alpha H_c t = \dot{Q}_o [tH^{3/2} g^{1/2}/A]^n \\ \dot{C}_{\text{CO}} &= \alpha \gamma t = \beta \dot{Q} \end{aligned} \quad (30)$$

where \dot{C}_{CO} is measured in g_{CO} per unit time. From the above it is concluded that $n = 1$; $\dot{Q}_o = \alpha A H_c / (H^{3/2} g^{1/2})$; $\beta = \gamma / H_c$ (31)

Also

$$\begin{aligned} H &= 2.11 \text{ m}, \Delta = 0.33 \text{ m}, g = 9.8 \text{ m/s}^2, A = 8.83 \text{ m}^2 \\ T_a &= 294^{\circ}\text{K}, \rho_a = 1.18 \text{ kg/m}^3, C_p = 240 \text{ cal/(kg}^{\circ}\text{K)} \end{aligned} \quad (32)$$

Radiant losses from the combustion zone are neglected, i.e., $\lambda_r = 0$. Considerations in the Appendix of Cooper⁹, together with experimental results of Mulholland et al.¹⁰, and Veldman et al.¹¹ indicate that for a $\lambda_r = 0$ combustion

zone in an enclosure with proportions similar to the present one, $\lambda_c \approx 0.6$. This λ_c value will be used here.

Using Eqs. (28), (29), (31) and (32) along with the above λ values in Eqs. (2) and (19) leads to

$$\phi = 135 M_{\text{cotton}} + 1 = 204 M_{\text{polyurethane}} + 1 \quad (33)$$

where, e.g., M_{cotton} is the upper layer concentration of CO during smoldering of the cotton source. Using the above data in the ϵ , τ , and σ definitions of Eqs. (2) and (19) leads to the following representations for these variables which happen to be valid for both the cotton and polyurethane tests

$$\epsilon = 1.6(10^{-4}), \tau = 4.1(10^{-3})t^{4/3}, \sigma = 2.8(10^{-8})t^2; \quad (t \text{ in seconds}) \quad (34)$$

Either Figure 3 or 5 provides both an estimate for the time, t_o , when the interface drops to the elevation of the combustion zone, and an estimate for the temperature, ϕ_o , of the upper layer at this time. Thus,

$$\left. \begin{array}{l} \epsilon = 1.6(10^{-4}) \\ n = 1 \end{array} \right\} \rightarrow \begin{array}{l} \epsilon^{1/3} \tau_o = 3.8 \text{ or } \sigma_o = 0.062 \\ \phi_o = 1.066 \end{array} \quad (35)$$

Using these results in Eqs. (33) and (34) leads to the estimates

$$\begin{aligned} t_o &= 1.5(10^3)\text{s} \\ M_{\text{cotton}}(t=t_o) &= 4.9(10^2) \text{ ppm CO} \\ M_{\text{polyurethane}}(t=t_o) &= 3.2(10^2) \text{ ppm CO} \end{aligned}$$

Also, the time when the interface would reach the floor elevation, $\zeta = -\delta = -0.156$, can be estimated from Eqs. (23) and (34), and from the $\sigma_o = 0.062$ result of (35).

$$\sigma(\zeta=-\delta) = \sigma_o + \delta = 0.218 \rightarrow t(\zeta=-\delta) = 2.8(10^3)\text{s}$$

Thus, the theory indicates that the interface reached the floor somewhat prior to the 60 minute duration of the tests.

With the use of the transformations of Eqs. (33) and (34), M_{cotton} and $M_{\text{polyurethane}}$ data¹² (sampling port 1.68 m above the floor) are plotted in Figure 8 up to the time $\sigma = 0.37$ [$t = 3.6(10^3)\text{s}$]. Also included in the figure are figure 4 type $\mu(\sigma)$ and $\zeta(\sigma)$ plots for $\epsilon = 1.6(10^{-4})$ and $n = 1$. As can be noted, there is excellent agreement between computed and measured values for μ . Relative to this agreement, however, it should be stressed that the measured

values for $\mu = \phi - 1 = T/T_a - 1$ are from CO concentration measurements rather than temperature measurements. Values for $T/T_a - 1$ which would correspond to actual measured temperatures¹² are less than an order of magnitude smaller than the indicated theoretical values. This is consistent with H_c estimates of Ohlemiller¹³, which are an order of magnitude smaller than the reference 8, H_c estimates of Eq. (28). Thus, for example, if the above calculation is carried through for polyurethane using $H_c = 1.5$ kJ/g instead of 15 kJ/g, then at 3600 s the predicted pairs of values for M and T/T_a are $1.9(10^3)$ ppm CO and 1.04 ($H_c = 1.5$ kJ/g) compared to $2.0(10^3)$ ppm CO and 1.4 ($H_c = 15$ kJ/g).

Hazard Development in Enclosures Containing Some Larger Scale Fires

Table 4-2 of reference 14 provides a catalogue of experimentally determined energy release rates obtained by Heskestad¹⁵ for the growth stages of flaming fires in practical fuel assemblies. The \dot{Q} of all items in this listing is proportional to t^2 . For example, the \dot{Q} of many items can be estimated by ($t_g = 1000$ s in the nomenclature of reference 14)

$$\dot{Q} = 0.10 t^2 \text{ kW/s}^2 \quad (t \text{ in seconds}) \quad (37)$$

These latter items include wood pallets stacked 3.0-4.6 m high, many different types of polyethylene, polypropylene, polystyrene and PVC commodities in cartons stacked 4.6 m high, and a horizontal polyurethane mattress.

The results of the present analysis will be used to characterize the hazard development in enclosures which contain Eq. (37)-type fires. Toward this end, Eqs. (1) and (37) lead to the result

$$n = 2; \dot{Q}_o = 0.010(A^2/H)\text{kW/m} \quad (38)$$

Using Eq. (38) in Eq. (2) together with the values of ρ_a , C_p , T_a and g of Eq. (32) leads to

$$\begin{aligned} \dot{Q}_o^* &= 9.4(10^{-6})A^2 H^{-11/2} m^{3/2}; \epsilon = 0.015(1-\lambda_c)(1-\lambda_r)^{-3/5} A^{4/5} H^{-11/5} m^{3/5} \\ \tau &= 0.085(1-\lambda_r)^{1/3} H^{2/3} A^{-1} t^{5/3} m^{4/3} s^{-5/3} \end{aligned} \quad (39)$$

With Eq. (39), the results of the present analysis can now be used to answer a wide variety of hazard related questions. For illustrative purposes two such questions will be addressed here.

Question 1:

Flaming ignition is initiated in stacked commodities of the "Eq. (37) variety" which are contained in a warehouse of height 6 m and area 1500 m². At what time does the upper layer attain the potentially untenable temperature¹ (due to downward radiation) of 183⁰C, and what is the elevation of the layer interface at this time?

Answer (Solution):

Consistent with recommendations in reference 2, assume $\lambda_r = 0.35$, and, for the purpose of a hazard analysis of this type, conservatively assumed $\lambda_c = 0.6$. Take H to be the floor-to-ceiling dimension, 6 m, and Δ to be zero. Then for $A = 1500 \text{ m}^2$, Eq. (39) leads to

$$\epsilon = 0.052; \tau = 1.6(10^{-4}) t^{5/3} \quad (\text{t in seconds}) \quad (40)$$

From the above, $T_{\text{hazard}} = 183^{\circ}\text{C} = 456^{\circ}\text{K}$ and $T_a = 294^{\circ}\text{K}$. Then for $\epsilon = 0.05$ and $n = 2$, Figure 4 and the τ, t transformation of Eq. (39) provides the result:

$$\phi = \phi_{\text{hazard}} = T_{\text{hazard}}/T_a = 1.55 \quad (41)$$

when

$$\begin{aligned} \tau = \tau_{\text{hazard}} &= 3.0 \rightarrow t_{\text{hazard}} = 370 \text{ s} \\ \zeta = \zeta_{\text{hazard}} &= 0.44 \rightarrow Z_1 = Z_{\text{hazard}} = 2.6 \text{ m} \end{aligned}$$

Thus, the hazardous condition will occur (no earlier than) 370 s following ignition, and when the layer interface is (no lower than) 2.6 m from the warehouse floor. Note from Eq. (37), that the strength of the fire at this time is estimated to be 14 MW.

Question 2:

Flaming ignition is initiated in a polyurethane mattress 0.6 m above the floor of a hospital ward with floor-to-ceiling dimension of 3 m and area 10 m². At what time does the upper layer interface reach the potentially hazardous 1.5 m elevation, and what is the upper layer temperature at this time?

Answer (Solution):

As in the previous solution, take $\lambda_c = 0.6$, $\lambda_r = 0.35$ and $T_a = 294^{\circ}\text{K}$. Also, $H = 2.4 \text{ m}$, $\Delta = 0.6 \text{ m}$, $Z_{\text{hazard}} = 0.9 \text{ m}$, and $A = 100 \text{ m}^2$. Then, from Eq. (39)

$$\epsilon = 0.045; \tau = 1.3(10^{-3}) t^{5/3} \quad (\text{t in seconds}) \quad (42)$$

As before, the $\epsilon = 0.05$, $n = 2$ plots of Figure 4 once again provide a basis for obtaining the desired solutions. Using these plots and the new τ , t transformation of Eq. (42) leads to the result:

$$\zeta_{\text{hazard}} = Z_{\text{hazard}}/H = 0.38$$

when

$$\begin{aligned} \tau = \tau_{\text{hazard}} &= 3.3 \quad \rightarrow \quad t_{\text{hazard}} = 110 \text{ s} \\ \phi = \phi_{\text{hazard}} &= 1.64 \quad \rightarrow \quad T_{\text{hazard}} = 482^{\circ}\text{K} = 209^{\circ}\text{C} \end{aligned}$$

Thus, the layer interface will drop to the 1.5 m elevation (no earlier than) 110 s following ignition, and its average (untenable) temperature will be (no higher than) 209°C . Note from Eq. (37) that the strength of the fire at this time is estimated to be 1.2 MW.

SUMMARY AND CONCLUSIONS

A set of general model equations which simulate the dynamic environment in enclosures containing fires has been previously formulated and reported in references 1 and 2. To use the model one must specify the energy release rate of the fire, certain heat transfer parameters, the area and height of the enclosure, and the elevation of the fire above the floor. If predictions of the concentration of a product of combustion is desired then the fire's rate of generation of that product must also be specified.

The present work has solved the model equations for the class of growing fires which can be characterized by energy release rates, \dot{Q} , which are proportional to t^n , where t is time and $n \geq 0$ is any fixed number. This class includes all constant energy release rate fires ($n = 0$), "ramp fires" ($n = 1$) and t^2 fires ($n = 2$). These descriptions of energy release rate have been used extensively in the literature to characterize the growth of fires in practical fuel assemblies which are common to a wide range of real building occupancies.

The model equations and the present solutions predict the time-varying temperature and thickness of a combustion product laden upper layer which, at the time of ignition, grows from zero thickness at the ceiling of the enclosure. General time-varying solutions for the variables, in the form of dimensionless working plots, have been presented in Figures 2-7.

For those fires which generate any specific product of combustion at a rate proportional to $\dot{Q} \sim t^n$, solutions have also been obtained for the upper layer concentration of that product. Plots of these are presented in Figures 3-7.

Specific results for the solution variables at the time, t_0 , when the upper layer interface reaches the fire elevation are presented in Figures 3 and 5. For the important special case of constant fires ($n = 0$), these latter results led to the remarkable conclusion, presented in Eq. (18), that t_0 is relatively independent of the fire-to-ceiling distance, H .

The results presented in this work can be used to solve a wide range of fire safety problems. In order to provide a hint of the utility of these results two types of example applications, one relating to smoldering combustion hazards and one relating to flaming combustion hazards, were presented. In the case of smoldering combustion, present results from the theory were compared to data which were previously acquired during two full scale experiments. In the case of flaming combustion the theory was used to predict the onset of hazardous conditions in both a hospital and a warehouse fire scenario.

The fire environment model equations solved here represent a compromise between accuracy in real fire environment simulation and practicality of implementation. In this regard it is reasonable to envisage future implementation of somewhat more modeling detail which would not seriously detract from the overall model practicality. For example, the use of a somewhat more detailed description of heat transfer phenomena (i.e., λ_c), as reported in references 15 and 16, would lead to more reliable upper layer temperature estimates. An accounting of significant upper layer-lower layer mixing due to wall effects would also lead to an important model improvement. Model improvements of this type are the focus of present investigations.

ACKNOWLEDGMENTS

This work was supported in part by the U.S. Department of Health and Human Services, and the Bureau of Mines and National Park Service of the U.S. Department of Interior.

REFERENCES

1. Cooper, L. Y., A Concept for Estimating Safe Available Egress Time in Fires, to appear in Fire Safety Journal.
2. Cooper, L. Y., A Mathematical Model for Estimating Safe Available Egress Time in Fires, to appear in Fire and Materials.
3. Cooper, L. Y., Measuring the Leakage of Door Assemblies During Standard Fire Exposures, Fire and Materials, Vol. 5, No. 4, 1981.
4. Cooper, L. Y., Calculating Escape Time from Fires, Proceedings of 1980 SFPE/NBS Workshop on Applications of Fire Technology, Soc. Fire Prot. Eng. publication.
5. Cooper, L. Y., Harkleroad, M., Quintiere, J., Rinkinen, W., An Experimental Study of Upper Hot Layer Stratification in Full-Scale Multiroom Fire Scenarios, 20th Nat'l. Heat Transfer Conf., Milwaukee, 1981, to appear in J. Heat Transfer.
6. Baines, W. D. and Turner, J. S., Turbulent Buoyant Convection from a Source in a Confined Region, Journal Fluid Mech., Vol. 37, Part I, 1969.
7. Zukoski, E. E., Development of a Stratified Ceiling Layer in the Early Stages of a Closed-Room Fire, Fire and Materials, Vol. 2, No. 2, 1978.
8. Quintiere, J., Birky, M., Smith, G., An Analysis of Smoldering Fires in Closed Compartments and Their Hazard Due to Carbon Monoxide, to appear in Fire and Materials.
9. Cooper, L. Y., Estimating Safe Available Egress Time from Fires - Appendix, NBSIR 80-2172, Nat'l. Bur. Stand., Feb. 1981.
10. Mulholland, G., Handa, T., Sugawa, O., Yamamoto, H., Smoke Filling in an Enclosure, 20th Nat'l. Heat Transfer Conf., Milwaukee, 1981.
11. Veldman, C. C., Kubota, T., and Zukoski, E. E., An Experimental Investigation of the Heat Transfer from a Buoyant Gas Plume to a Horizontal Ceiling - Part 1. Unobstructed Ceiling, Calif. Inst. Tech. Rept. NBS-GCR-77-97, prepared for U.S. Dept. of Commerce, Nat'l. Bur. Stand., 1975.
12. Smith, G., Research Associate (1981), National Bureau of Standards, private communication.
13. Ohlemiller, T., National Bureau of Standards, private communication.
14. NFPA 204M Guide for Smoke and Heat Venting, National Fire Protection Assoc., 1982.
15. Heskestad, G., Factory Mutual Research Corp., private communication.

16. Cooper, L. Y., Convective Heat Transfer from a Buoyant Plume to an Unconfined Ceiling, J. Heat Transfer, Vol. 104, No. 3, 446-451, 1982.
17. Cooper, L. Y., Convective Heat Transfer to Ceilings Above Enclosure Fires, 19th Inter. Symp. on Combustion, Haifa, 1982.

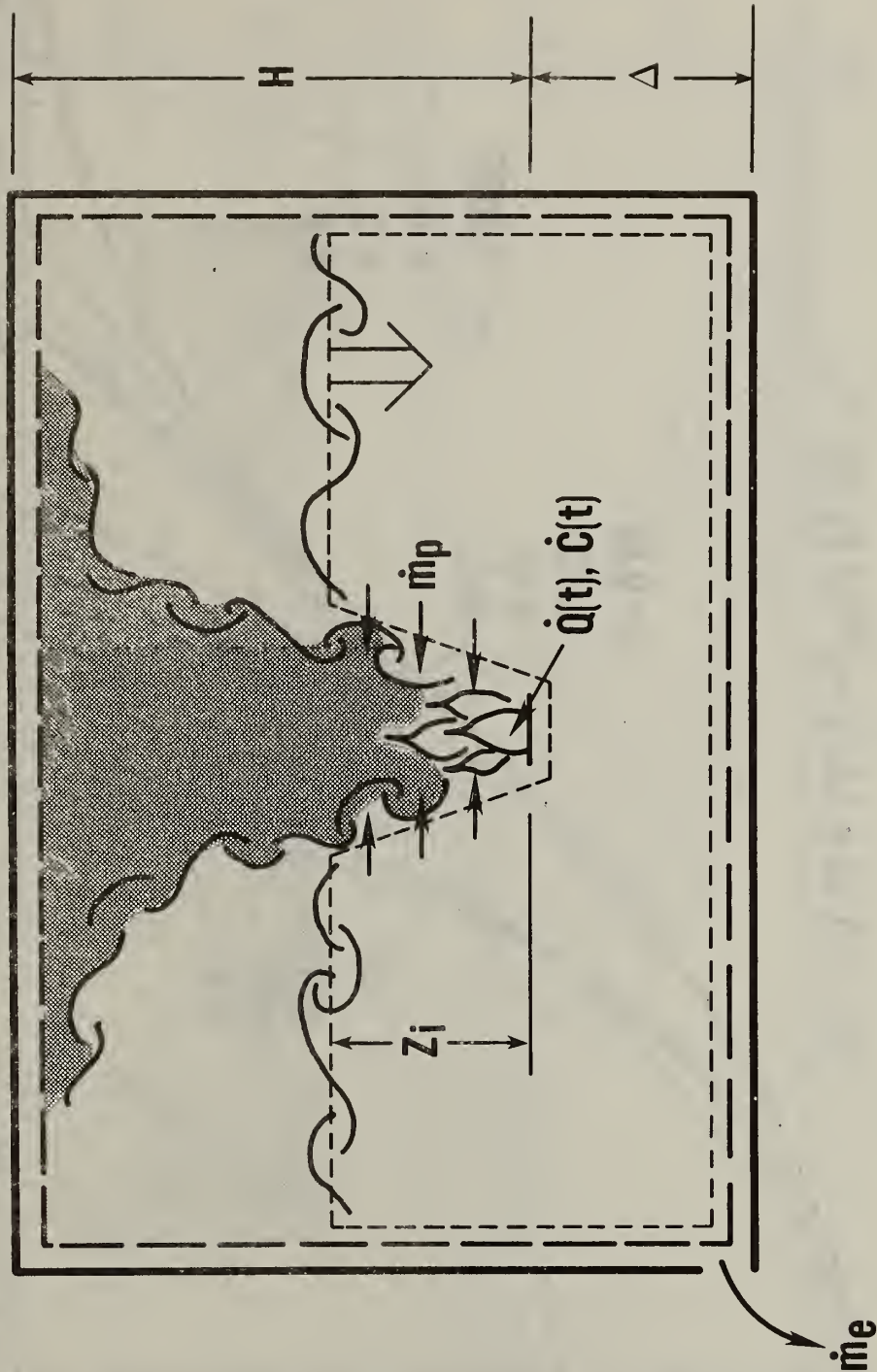


Figure 1. Fire-in-enclosure flow dynamics consistent with the model .

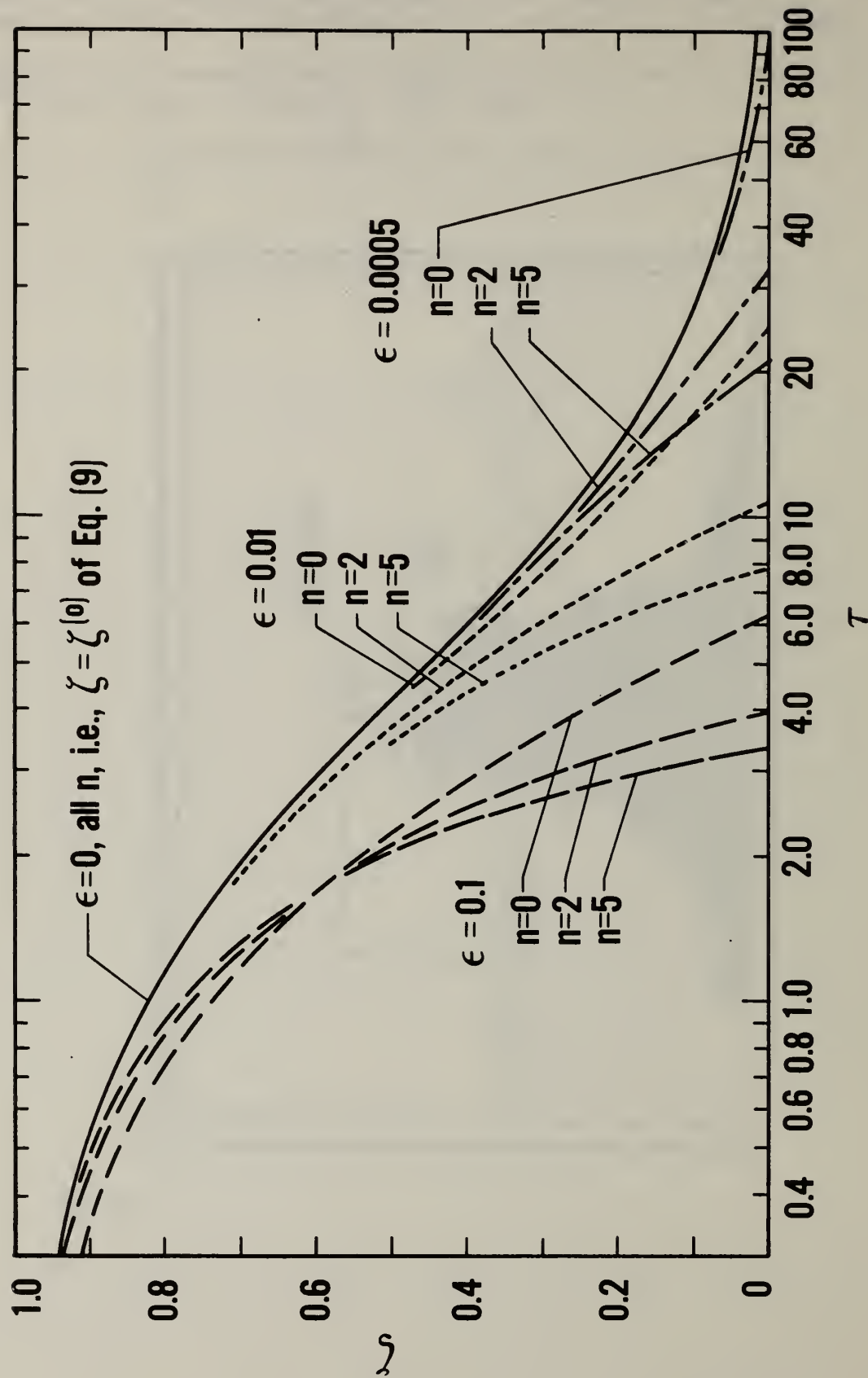


Figure 2. Plots of $\zeta(\tau)$ for different values of n and ϵ , $0 < \tau \leq \tau_0$.

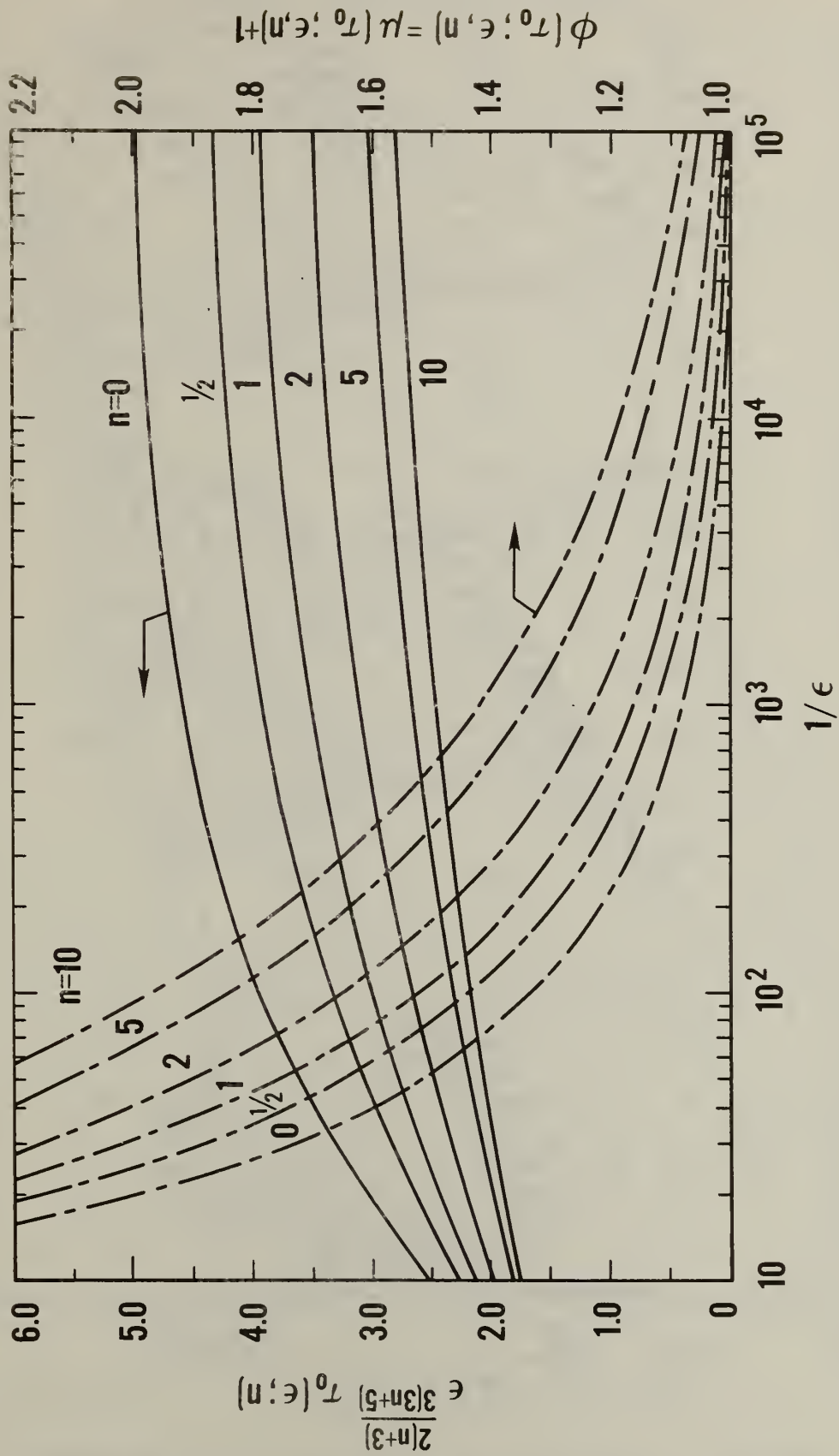


Figure 3. Plots of $\epsilon^{2(n+3)/[3(3n+5)]} \tau_0$ and ϕ_0 as functions of $1/\epsilon$ for different values of n .

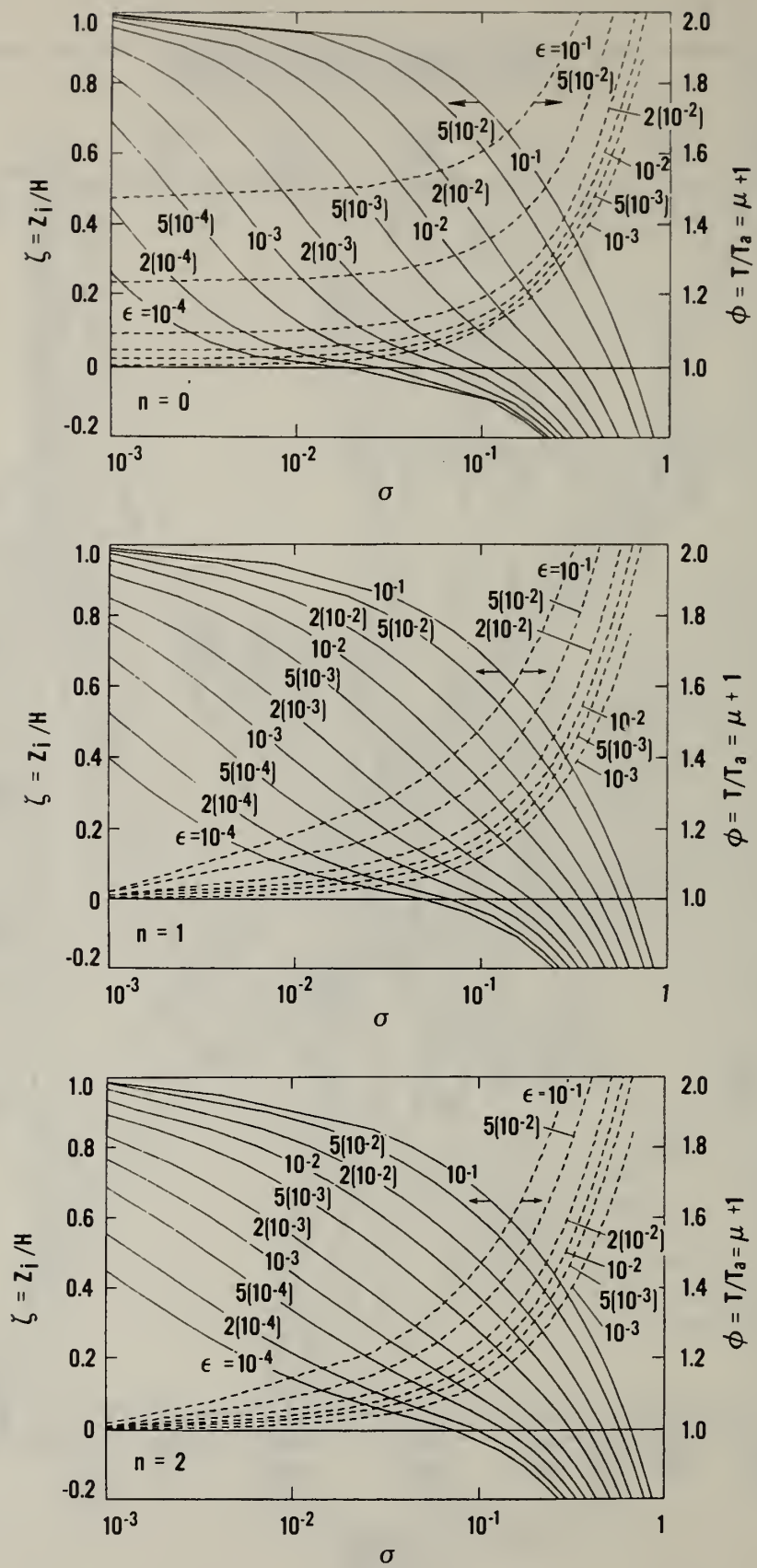


Figure 4. Plots of $\zeta(\sigma)$ and $\phi(\sigma)$, $0 < \zeta < 1$, for different values of ϵ , and for $n = 0$, $n = 1$, and $n = 2$.

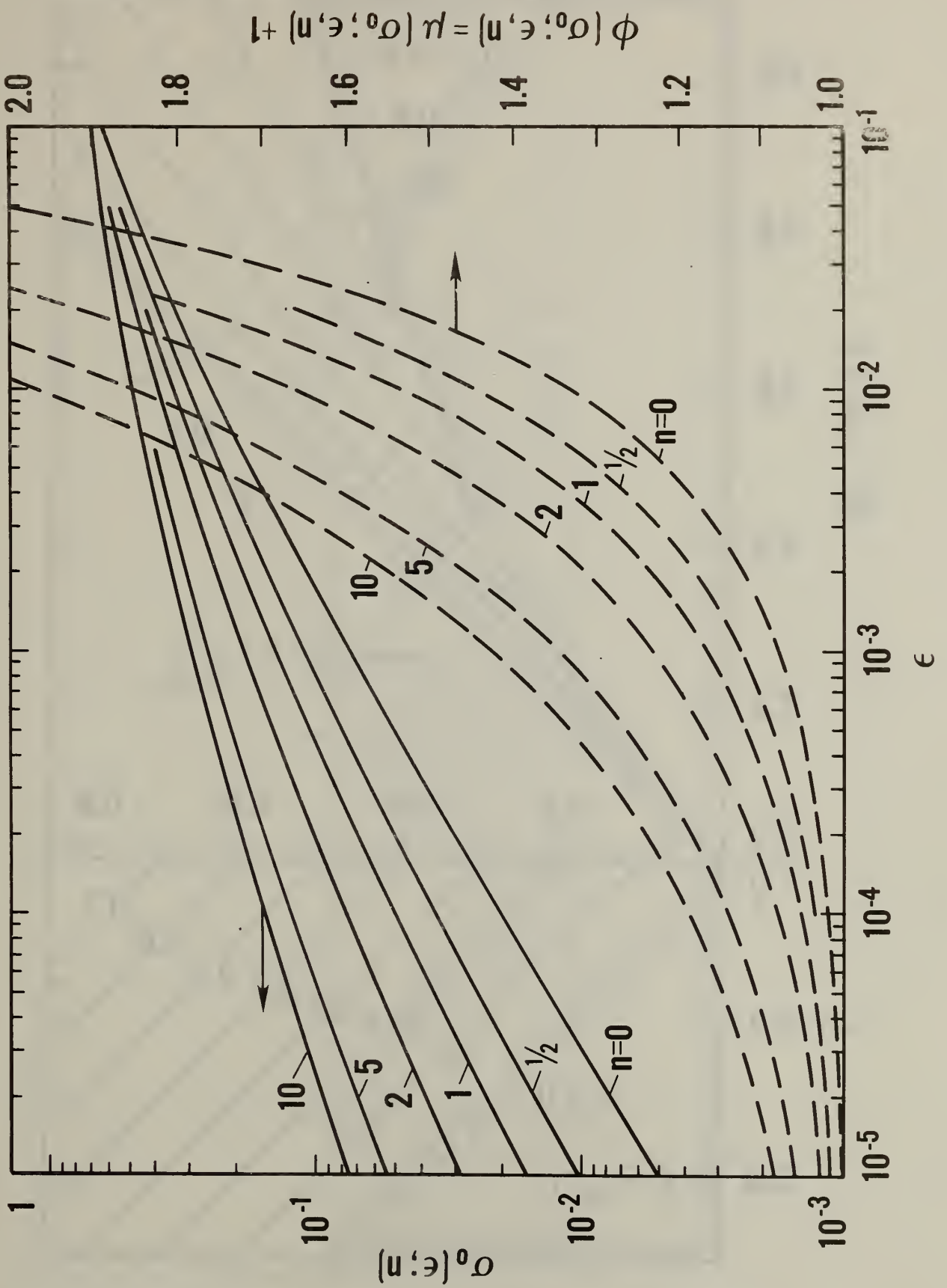


Figure 5. Plots of $\sigma_0(\epsilon)$ and $\phi_0(\epsilon)$ for different values of n .

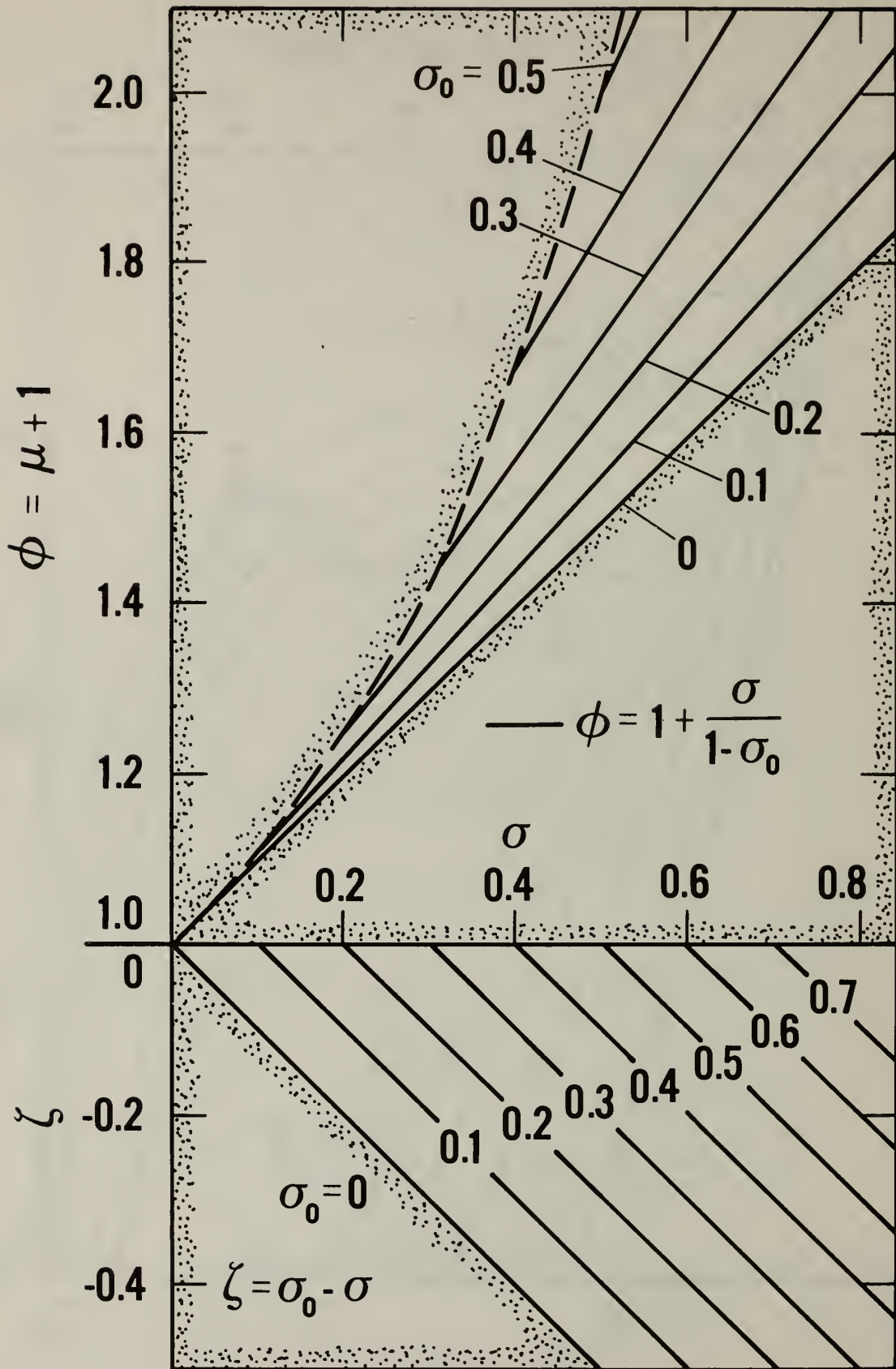


Figure 6. Plots of $\zeta(\sigma)$ and $\phi(\sigma)$, $-\delta < \zeta \leq 0$, for different values of σ_0 .

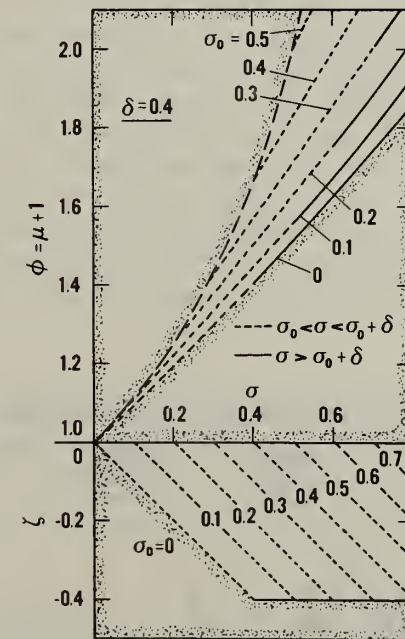
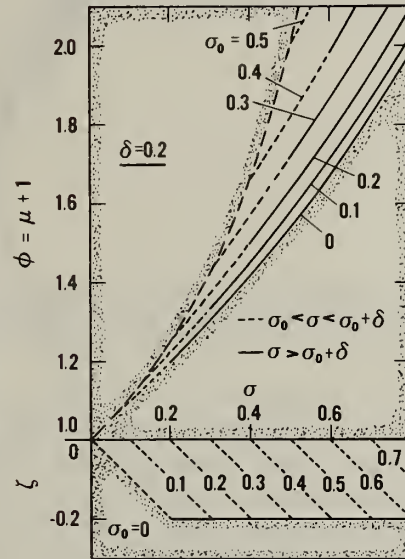
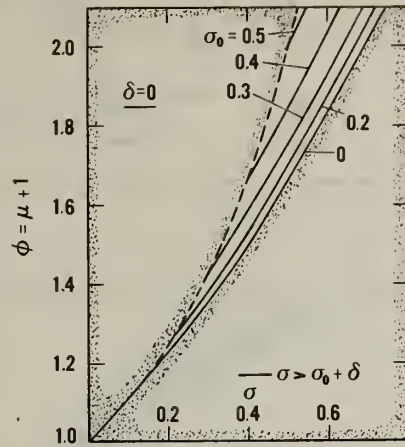


Figure 7. Plots of $\zeta(\sigma)$ and $\phi(\sigma)$, $\zeta \leq 0$, for different values of σ_0 , and for $\delta = 0$, $\delta = 0.2$, and $\delta = 0.4$.

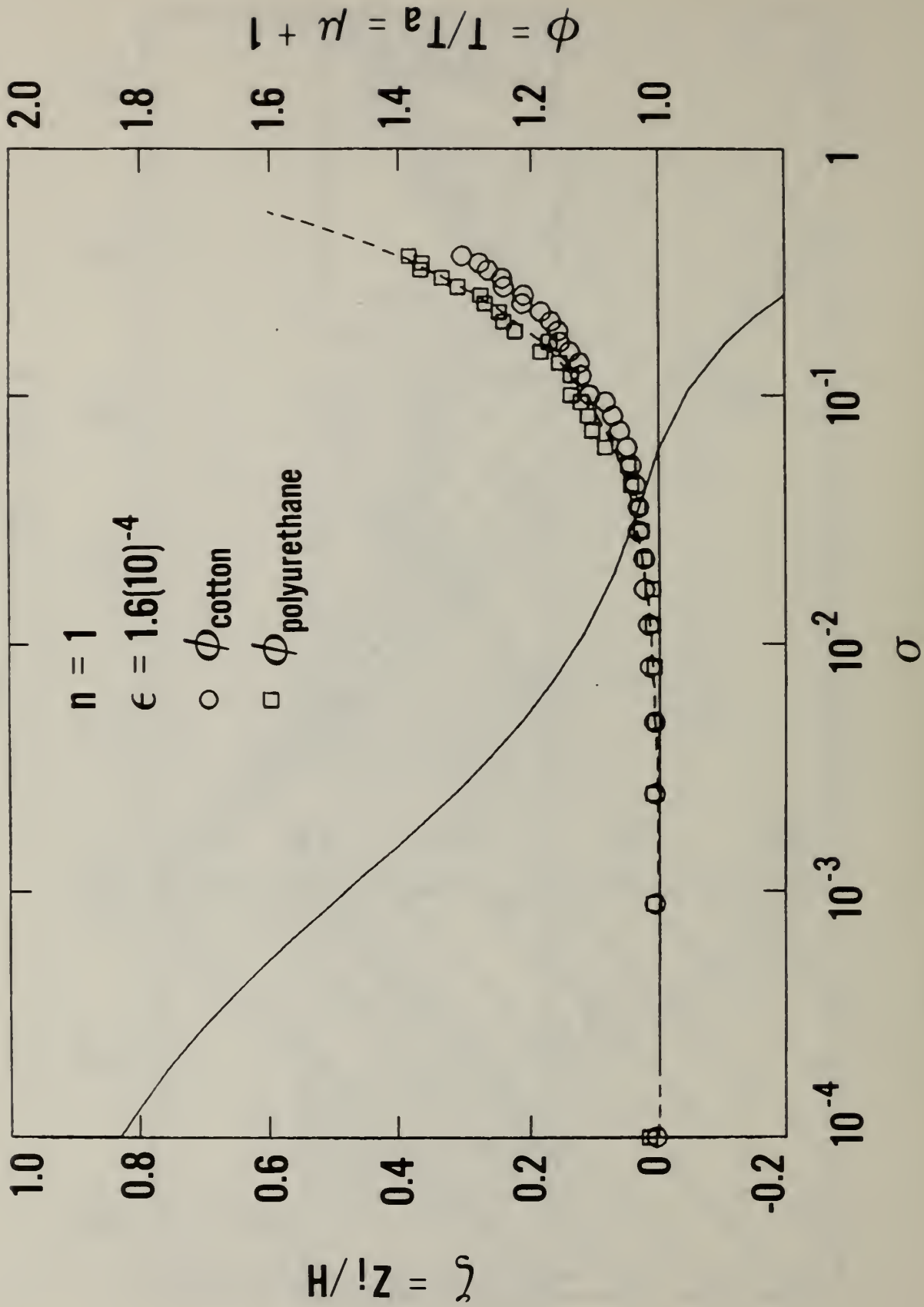


Figure 8. Plots of $\zeta(\sigma)$ and $\phi(\sigma)$ for $n = 1$ and $\epsilon = 0.00016$, and plots of μ_{CO} data from cotton and polyurethane smoldering experiments.

| | | | |
|---|---|------------------------------------|---|
| U.S. DEPT. OF COMM. BIBLIOGRAPHIC DATA SHEET <i>(See instructions)</i> | 1. PUBLICATION OR REPORT NO. NBSIR 82-2622 | 2. Performing Organ. Report No. | 3. Publication Date January 1983 |
| 4. TITLE AND SUBTITLE THE DEVELOPMENT OF HAZARDOUS CONDITIONS IN ENCLOSURES WITH GROWING FIRES | | | |
| 5. AUTHOR(S) Leonard Y. Cooper | | | |
| 6. PERFORMING ORGANIZATION <i>(If joint or other than NBS, see instructions)</i> NATIONAL BUREAU OF STANDARDS DEPARTMENT OF COMMERCE WASHINGTON, D.C. 20234 | | 7. Contract/Grant No. | 8. Type of Report & Period Covered FINAL |
| 9. SPONSORING ORGANIZATION NAME AND COMPLETE ADDRESS <i>(Street, City, State, ZIP)</i> | | | |
| 10. SUPPLEMENTARY NOTES <input type="checkbox"/> Document describes a computer program; SF-185, FIPS Software Summary, is attached. | | | |
| 11. ABSTRACT <i>(A 200-word or less factual summary of most significant information. If document includes a significant bibliography or literature survey, mention it here)</i> A mathematical model for simulating the environment in enclosures during the growth stage of hazardous fires was developed previously. To use the model one must specify the energy release rate of the fire, certain heat transfer parameters, the area and height of the enclosure and the elevation of the fire above the floor. Solution to the model's equations would yield the time-varying thickness, temperature, and product of combustion concentrations of an upper smoke layer which starts to drop from the enclosure ceiling at the time of ignition. In this paper the model equations are solved for the general class of fires whose energy release rate, \dot{Q} , and product of combustion generation rates, \dot{C} , are approximately proportional to t^n (t is time and $n \geq 0$). For such fires, general results for the complete solution history of the enclosure environment are obtained and presented in the form of graphs, and where possible, by closed form analytic expressions. Use of the results is illustrated in two example problems. The first of these involves a problem in smoldering combustion where, according to experimental data, the combustion zone can be simulated by an $n=1$ fire. The second involves a prediction of the environment produced in an enclosure which contains an $n=2$ fire, which simulates a specific, large-scale, flaming fire hazard. | | | |
| 12. KEY WORDS <i>(Six to twelve entries; alphabetical order; capitalize only proper names; and separate key words by semicolons)</i> Combustion products; compartment fires; egress; enclosure fires; fire detection; fire growth; hazard analysis; mathematical models; room fires; smoke movement; tenability limits. | | | |
| 13. AVAILABILITY <input checked="" type="checkbox"/> Unlimited <input type="checkbox"/> For Official Distribution. Do Not Release to NTIS <input type="checkbox"/> Order From Superintendent of Documents, U.S. Government Printing Office, Washington, D.C. 20402. <input checked="" type="checkbox"/> Order From National Technical Information Service (NTIS), Springfield, VA. 22161 | | 14. NO. OF PRINTED PAGES 32 | 15. Price \$7.50 |

